Radiation Physics and Chemistry xxx (xxxx) xxx–xxx

Contents lists available at ScienceDirect

Radiation Physics and Chemistry

journal homepage: www.elsevier.com/locate/radphyschem

Comparative analysis of the transmission properties of tissue equivalent materials

Bruna C. Nascimento[a,*], Audrew Frimaio[b], Ramon M.M. Barrio[a], Ana C.A. Sirico[a], Paulo R. Costa[a]

[a] Instituto de Física/Universidade de São Paulo, São Paulo, Brazil
[b] Instituto de Pesquisas Energéticas e Nucleares, São Paulo, Brazil

ARTICLE INFO

Keywords:
Tissue equivalent materials
Archer's equation
Transmission measurements

ABSTRACT

Phantom objects have as main requirement to have the effective atomic number and linear attenuation coefficient approximately equal to the human tissue to be simulated. The present work aims to characterize samples of materials radiologically equivalent to water for dose studies in patients in the diagnostic energy range. Water was chosen as reference material representing human tissue, which is composed mostly of it. A set of samples was formulated and submitted to radiation transmission tests in four different values of tension applied to an X-ray tube. Mass densities of the samples were evaluated using the Arquimedes method. The samples were identified as A, B, C and D. By transmission curves, it was possible to estimate the samples transmission factors corresponding to the water transmission factor for different thicknesses. Moreover, the thicknesses of samples equivalent to water thickness for different values of transmission factor were also evaluated. All the samples densities were bigger than the density of water. For the same thickness of water and the samples, the radiation transmission of the developed materials are in better agreement for thicknesses of 10 mm and 30 mm. The lowest percentage difference between the water transmission and the transmission of any of the samples obtained was approximately 0.6% for the sample A in the thickness of 30 mm under voltage of 60 kV. The correspondence between the transmission factors and the thicknesses showed that the compounds studied in this work are potential materials to develop phantoms that simulate the transmission properties of human tissue.

1. Introduction

Anthropomorphic phantoms have been developed to simulate the human body in the evaluation and calibration of the performance of imaging devices and to ensure appropriate dose in radiotherapy treatment (Dewerd and Lawless, 2014). This kind of object has been widely used in Quality Control (QC) and dosimetry evaluation of diagnostic imaging equipment (IAEA, 2007; IAEA, 2011). The materials used to design these objects have as main requirement to have the effective atomic number and linear attenuation coefficient approximately equal to the tissue to be simulated, in order to reproduce its characteristics of attenuation to the incident ionizing radiation (ICRU, 1989; Frimaio, 2017).

X rays are absorbed and scattered in different ways depending on the region of the human body and this has to be taken into account on the construction of simulator objects (Fisher, 2006). The equivalence between a phantom material and human tissue also depends on the range of energy applied to the X-ray tube, because the probability of occurrence of photoelectric effect depends strongly on the energy. The effective atomic number is the quantity related to this interaction characteristic (Prasad et al., 1997; Taylor et al., 2012; Saito and Sagara, 2017). The electron density is also important, since it impacts the probability of interactions by Compton effect (Shrimpton, 1981; Manohara et al., 2008).

A material widely used as a basis on development of phantoms is water. Water represents a significant fraction of the human body and mimics its radiation absorption and attenuation. However, as the chemical composition of the body changes according to the age (ICRU, 1989), the percentage of water in humans of different ages has to be take into account in the development of a phantom. In prenatal life, the total body water of a fetus vary from 95% to 70% as the fetus grows. For a newborn the average total body water is about 75%, but in few days after birth it decreases to about 60%. Finally, in the growth period and adult life the total body water decreases progressively with age. For men there's an exception during young adulthood, when the total body water has a small rise (ICRP, 1975).

In this way, water is very useful in phantom development. It can be used both as comparison parameter, instead of human tissue itself, or as

* Corresponding author.
E-mail address: bruna.costa.nascimento@usp.br (B.C. Nascimento).

https://doi.org/10.1016/j.radphyschem.2019.04.050
Received 14 December 2018; Received in revised form 22 April 2019; Accepted 23 April 2019
Available online 27 April 2019
0969-806X/

the phantom material. However, liquid water is not an appropriate phantom material for all kind of researches and routine tests in real diagnostic imaging equipment. Therefore, other solid materials are more indicated on phantoms construction, such as polystyrene and acrylic (Constantinou et al., 1982). These materials are already available in the market and they are used when the need of high similarity between the target-tissue and the phantom material is not important, since their equivalence to most of the human body tissue is only a roughly approximation. In cases when a higher accuracy is required, another way to construct phantoms is developing and validating specific materials taking into account the clinical applications and the level of similarity required to comply to these needs (Amini et al., 2018).

Brazilian know-how and technology development in this field is growing in the last years, but it is not totally established (Costa, 2015). Besides that, even the materials available in international market were not properly evaluated for a good representation of the attenuation and scattering properties of ionizing radiation in the range energy used in diagnostic imaging (5–150 keV). The recent literature shows that phantoms are being developed for different uses, like evaluation of 2D and 3D breast-imaging systems (Ikejimbaa et al., 2017) and for simulation of dedicated breast CT perfusion imaging (Caballo et al., 2018). The study of phantoms materials is also an object of interest of the medical physics works. New materials, like gelatin-based materials (Dahal et al., 2018), are being developed and production techniques already known, like 3D printing (Filippou and Tsoumpas, 2018), are being enhanced.

The goals on developing national phantoms is to make this technology more available and to promote the widely application of QC and dosimetry procedures, especially in developing countries. The local design and production of human tissue equivalent materials will reduce costs and time of acquisition of these devices for quality control and radiological protection professionals, improving theses services.

Authors of the present work are formulating compounds and prototypes from a computational algorithm developed in previous work (Kimura et al., 2011; Mariano, 2017; Mariano and Costa, 2017) to supply the need of this type of material using an innovative approach (Frimaio, 2017).

2. Materials and methods

2.1. Equivalent material samples

The chemical compositions of the equivalent material samples were established by the application of the methodology developed by Mariano and Costa (2017). It was used different additives such as calcium carbonate ($CaCO_3$, Purity: 98%) and titanium dioxide (TiO_2, Purity: 99%) obtained from Basile Química Ltda (São Paulo, Brazil), calcium difluorite (CaF_2, Purity: 99%) from ABC-Lab Produtos e Equipamentos para Laboratórios (São Paulo, Brazil), and magnesium oxide (MgO, Purity: > 99%) from Labsynth (São Paulo, Brazil). The mixture of these compounds was in order to make the effective atomic number of the samples closest to the effective atomic number of the target material. The thickness of the samples, the electron density of the samples, the effective atomic number (Z_{eff}) of the samples and the chemical element composition of the materials are presented in Table 1.

These samples intended to be water-equivalent in terms of radiation transmission of X-ray beams in the range of energy between 15 and 150 keV. As a preliminary study, a set of samples were produced in order to evaluate the radiation attenuation provided by a determined thickness. Therefore, these samples were produced in plate format, without any concern with an anthropomorphic geometry of specific dosimetry or QC application. In order to increase accuracy, four different sets of resin compounds were designed in 30 × 20 cm^2 plates that were cut into sets of six pieces of 10 × 10 cm^2. The samples were cut with similar shapes and thicknesses to achieve similar radiation attenuation conditions. For convenience, the samples were identified as A, B, C and D. The samples' thicknesses were determined by a caliper rule (530-104BR, Mitutoyo) and the measurement uncertainties were estimated as half of the smallest measure.

2.2. Experimental configuration to transmission properties measurements

In order to compare the transmission properties of the slabs of the developed water-equivalent materials and the liquid water, an X-ray transmission experiment was conducted. In this experiment, an X-ray tube irradiated different thicknesses of the four samples and of water. The X-ray tube (SMART 300HP, YXLON, Germany) has a tungsten anode and can operate in a voltage range between 50 kV and 300 kV and currents between 0.5 mA and 3.0 mA. It was applied an additional filtration to represent a beam quality of RQR5 (IAEA, 2007). A filter of 2.58 mm of Aluminium was used. Voltages of 60 kV, 80 kV, 100 kV and 120 kV were applied to the X-ray tube for the radiation transmission tests. These values of voltage were chosen to cover a typical diagnostic imaging energy range. For the tests with voltage of 60 kV it was applied a current of 1.7 mA and for the others values it was applied a current of 3.0 mA. Transmitted radiation were measured using an ionization chamber (TW 23361, PTW, Inc., Germany). The chamber has 30 cm^3 of volume and it was calibrated by a SSDL national laboratory (IAEA, 2007).

The plates were placed over an acrylic structure. They were stacked one by one. To each new plate stacked it was obtained a bigger thickness and the transmission test was done. Five measurements were performed for each thickness of each sample in each of the applied voltages. For comparison, different water thicknesses were submitted to the same attenuation tests as the samples with equal beams. For these tests the volume of water was placed in an acrylic container of square section with the same area of the samples. Fig. 2 presents the experimental configuration adopted.

2.3. Transmission properties

The transmission properties of the samples and water to each value of voltage used in experiments were evaluated using the Archer Model (Archer et al., 1983, 1994; Burguer et al., 2011; Costa and Caldas, 2002; Santos et al., 2015). This mathematical model was created from the National Council on Radiation Protection and Measurements data to fit attenuation curves of radiation transmitted in X-ray rooms in order to standardize the calculation of the thickness necessary to protect an X-ray room. The correspondence between the fit and experimental curves is excellent. The fit of transmission in relation to thickness is calculated using the following equation:

Table 1
Physical and chemical characteristics of the samples A, B, C and D.

Samples	Thickness (mm)	Z_{eff}	Electronic density (e^-/cm^3)	Chemical elements composition
A	12.0 ± 0.7	6.70	3.60	C(0.3263); H(0.4900); O(0.1726); Mg(0.0100)
B	10.8 ± 0.7	7.03	3.58	C(0.3296); H(0.4950); O(0.1709); Ti(0.0033)
C	10.0 ± 0.7	7.07	3.59	C(0.3321); H(0.4950); O(0.1693); Ca(0.0025
D	10.1 ± 0.6	7.01	3.59	C(0.3296); H(0.4950); O(0.1643); Ca(0.0033); F(0.0066)

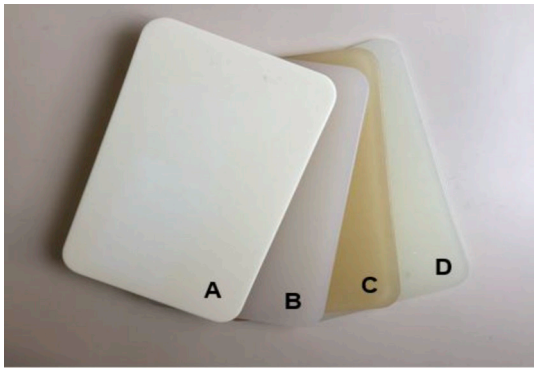

Fig. 1. Tissue equivalent resin-based samples A, B, C and D.

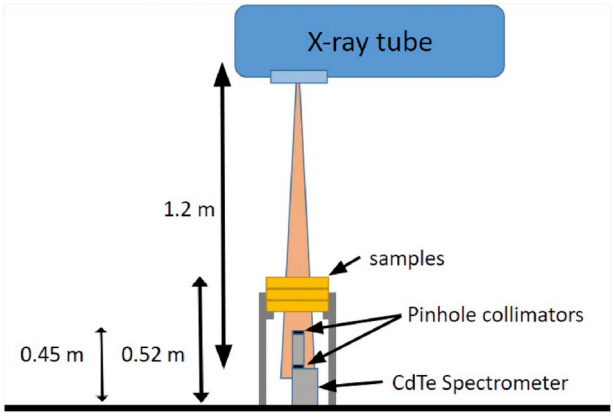

Fig. 2. Schematic diagram of the experimental set-up used.

$$B(x) = \left[\left(1 + \frac{\beta}{\alpha}\right)e^{\alpha\gamma x} - \frac{\beta}{\alpha}\right] \quad (1)$$

In the equation, $B(x) = \frac{K(x)}{K(0)}$ represents the transmission factor of the radiation through a thickness x of the material, where $K(x)$ is kerma transmitted in air through a thickness x and $K(0)$ is kerma transmitted in air without attenuation. α, β and γ are fitting parameters obtained using Levemberg-Macquardt method and depend on kVp.

2.4. Samples densities

The densities of the samples were determined in order to analyse the equivalency between the differents materials and water. A triangular piece of each one of the samples sets was cut and their masses were measured by two equal analytical balances (AE 200, Mettler-Telode (HK) MTCN Limited, Kowloon, Hong Kong). The variation between the values was in the order of 10^{-3}%, so only one measurement in each balance was necessary. Masses values were defined as the mean of the two values with uncertainties equal to standard deviation.

To measure volume, a beaker was filled with distilled water and its mass was determined by the same balances, which were reset to zero with the beaker full on them. The samples pieces were tied by a nylon wire and submerged in the beaker. Then, the balances measured dislocated distilled water mass. The dislocated distilled water volume was determined by:

$$V = \frac{m}{d} \quad (2)$$

where V is volume, m is mass and d is density.

Distilled water density value $d = 0.9969(1)g/cm^3$ was obtained by a table given by Didactic Laboratory of Institute of Physics of University of São Paulo. This process was repeated 5 times in each piece in the two balances. Using eq. (2), it was possible to determine the samples densities. The volume of nylon wire was estimated and the value was incorporated to the results.

3. Results and discussion

3.1. Transmission curves for the different samples and water

Graphics of the transmission curves separated by material (including water) are shown in Fig. 3. The fluctuation between the five measures made for each thickness were about 2%. Therefore, the uncertainties of the transmission factor measurements were not visible in the graphics. In this form of representation it was possible to observe that for all samples the higher the applied voltage on the X-ray tube, the higher the transmission factor values for each thickness. This is an indicative of the direct proportionality between the energy of the photons and their penetration in the evaluated material. Moreover, at 120 kV, it was observed a slight behavior change of the transmission curve for sample C.

3.2. Transmission curves for the different tensions applied to the X-ray tube

Fig. 4 shows four graphics that represents the radiation transmission curves of all samples and water for each one of the tensions applied to the X-ray tube. The results indicated that water presents higher values of transmission factor along the studied thicknesses, which shows that the samples transmit less radiation than water in theses values of tension.

Table 2 contains the parameters, and obtained by the application of eq. (1) on the transmission curves of all the samples in all voltages. This equation was adjusted by the Levenberg-Maquardt method using software Origin 9.1 (OriginLab Co., Northhampton, MA). The large uncertainties of the Archer parameters are justified by the small number of measurements made for each sample at each voltage. These values were used to make a comparative analysis between the radiation transmission of the samples and of water.

3.3. Comparison between the radiation transmissions

The comparison between the radiation transmissions was calculated by dividing the transmission of a sample by the transmission of the water (Eq. (1)). Fig. 5 shows the results for thicknesses of 10 mm, 30 mm and 60 mm.

The ratio that has the closest value to 1 was considered to be the most suitable for the determined values of thickness and tension evaluated. For the three thicknesses studied, sample A shows the best results of equivalency between the transmissions. For a thickness of 10 mm, all the samples differ less than 10% from water in terms of transmission. For the other two thicknesses studied, the samples differed by up to 20% of the water transmission. Sample B and C showed an atypical behavior pattern at 120 kV voltage for all the thicknesses. This behavior was probably caused by a measurement error, since it was observed only at this voltage value.

It was noticed that the developed materials are more equivalent to water in terms of radiation transmission for the two smaller values of thicknesses studied. The lowest percentage difference between the water transmission and the transmission of any of the samples obtained was approximately 0.6% for the sample A in the thickness of 30 mm under tension of 60 kV.

3.4. Comparison between the thicknesses

To determine the samples thicknesses that correspond to water thickness, the curves of Fig. 4 were analysed for three values of transmission factors: 0.4, 0.6 and 0.8. The samples thicknesses were divided by the water thickness necessary to represent each one of these three factors (Table 3). Again, the values closest to 1 were considered to be

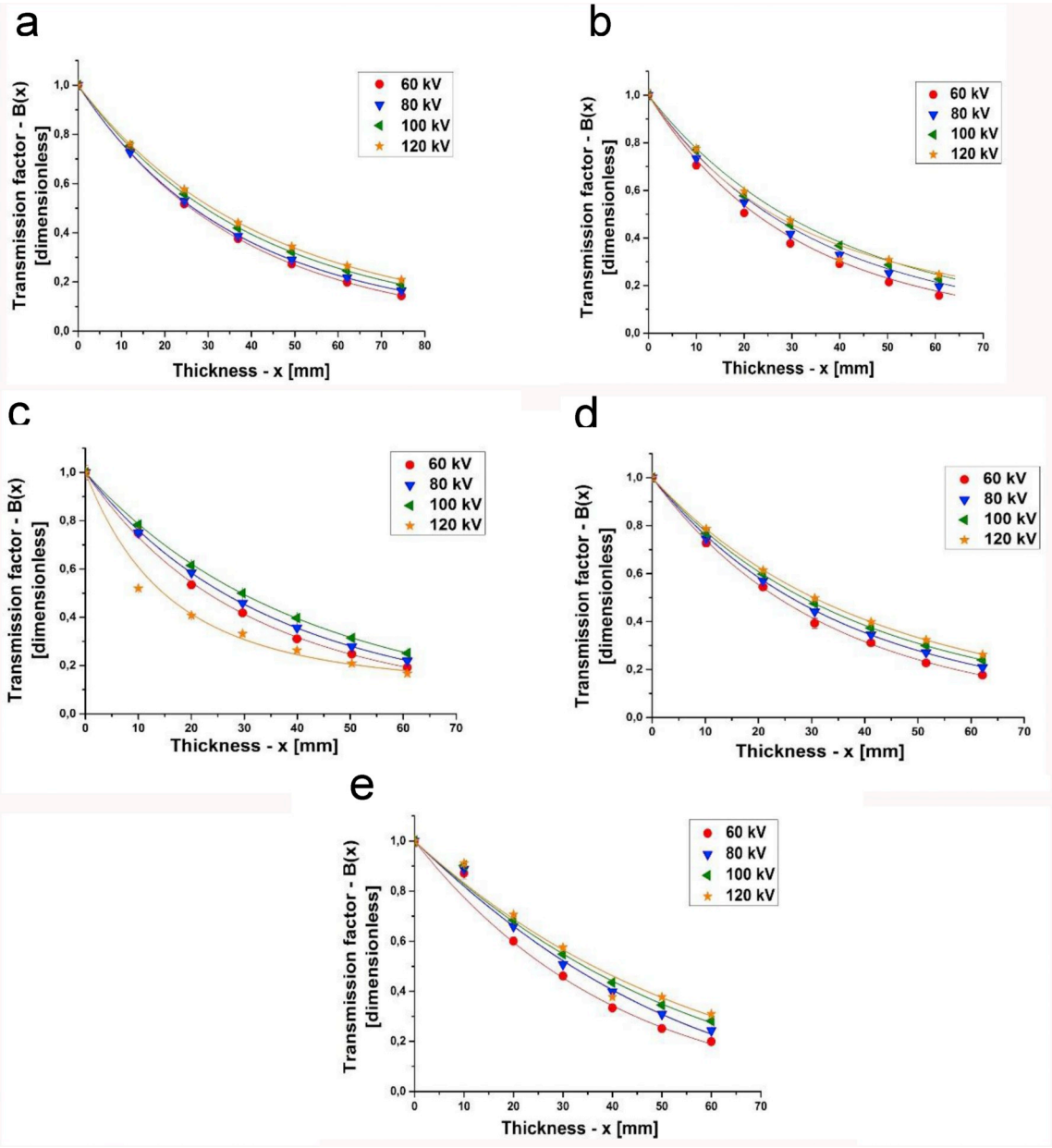

Fig. 3. Transmission curves for the four values of tension applied to the X-ray tube for (a) sample A, (b) sample B, (c) sample C, (d) sample D and (e) water.

indicators of greater agreement between the thicknesses. According to the reports of the table, the equivalency between the thicknesses is higher for the two lower transmission factors values for all the samples. The thicknesses of sample A and sample D are in better agreement with the water thickness in all voltages. For higher voltages (100 kV and 120 kV) sample C differ more from water and for low voltages (60 kV and 80 kV) the one that most differed was sample B.

3.5. Density of the samples

The densities values obtained are listed on Table 4. All the samples have densities bigger than the density of water. It shows that it is always necessary a lower thickness of sample to represent a thickness of water for the same transmission factor.

3.6. Study limitations

The limitations of the study were about the energy range and the basis of the materials used in the production of the samples. It was only studied the energy range used in diagnostic image (5–150 keV). In terms of the material, the manipulation of the based-material used in the production of the prototypes was a limiting factor. Besides that, the basis of the material were of epoxy resin only. Other samples with polimeric basis are in evaluation.

3.7. Comparative evaluation

Several studies can be find in the literature with information qualifying different tissue-equivalent materials in terms of their physical properties. Previous works shows results since very complex materials to be adopted in modern and sophisticated technologies to simple solutions useful for current clinical applications (Tomal and Costa, 2017).

Considering the importance on accurate dose and image quality evaluations in breast imaging, several works have been published in order to present phantoms which can be adopted in this modality. In a recent work, Glick&Ikejimba (Glick and Ikejimba, 2018) presented

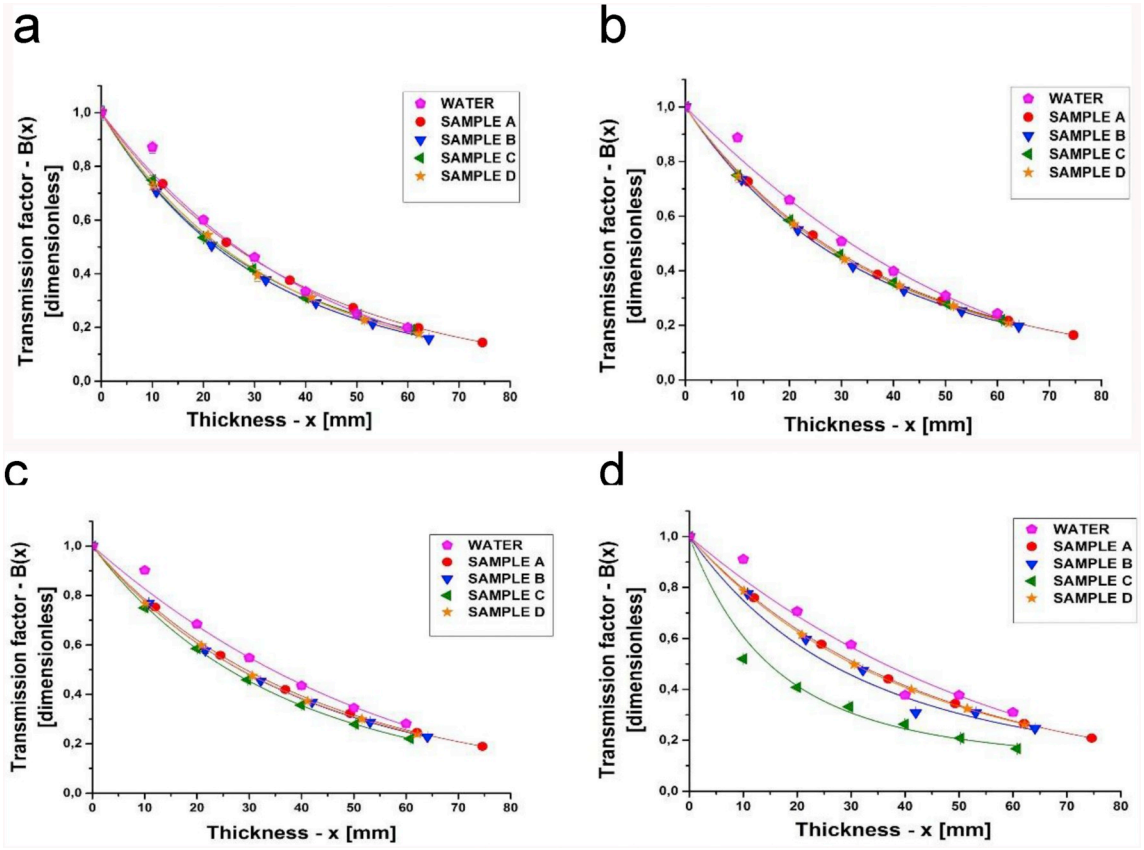

Fig. 4. Transmission curves for all the samples and for water for the four values of tension applied to the X-ray tube: (a) 60 kV, (b) 80 kV, (c) 100 kV and (d) 120 kV.

Table 2
Parameters obtained from the fit of Archel Model to the experimental data of all samples for all voltages.

Sample A				
	60 kV	**80 kV**	**100 kV**	**120 kV**
α	0.7(1.6)	0.9(4)	0.9(7)	0.9(4)
β	−0.6(1.6)	−0.8(4)	−0.8(7)	−0.9(4)
γ	−0.002(13)	−0.004(3)	−0.003(5)	−0.003(3)
Sample B				
	60 kV	**80 kV**	**100 kV**	**120 kV**
α	0.8(1.8)	0.8(3)	1.2(1.3)	0(7)
β	−0.8(1.8)	−0.8(3)	−1.2(1.3)	0(7)
γ	−0.005(2)	−0.005(3)	−0.003(6)	0.1(2.1)
Sample C				
	60 kV	**80 kV**	**100 kV**	**120 kV**
α	0.3(2.2)	0.7(9)	1.0(1.4)	3(8)
β	−0.3(2.2)	−0.7(9)	−0.9(1.4)	−3(8)
γ	−0.02(20)	0.005(10)	−0.002(9)	−0.01(3)
Sample D				
	60 kV	**80 kV**	**100 kV**	**120 kV**
α	0(3)	0.6(1.2)	0.4(9)	0.4(4)
β	0(3)	−0.6(1.2)	−0.4(9)	−0.3(4)
γ	0(7)	−0.006(2)	−0.01(4)	−0.011(18)
Water				
	60 kV	**80 kV**	**100 kV**	**120 kV**
α	0(18)	0(5)	0.4(6.2)	0(33)
β	0(18)	0(5)	−0.3(6.2)	0(33)
γ	0.01(6)	0.02(24)	0.01(15)	0(4)

several solutions associating digital and physical anthropomorphic breast phantoms for x-ray imaging. The authors studied the main available purposes for each kind of phantom given emphasis on the advantages and disadvantages present with each approach. Moreover, breast phantom technologies have been focused in searching solutions for realistic models of the breast. An example of a very creative solution was presented by Ikejimba et al. (Ikejimbaa et al., 2017). The authors proposed an accurate, inexpensive, easily accessible, method to fabricate any virtual phantom using an inkjet printer and parchment paper and a radiopaque ink in order to construct different breast models.

In terms of manufacturing technologies, the literature has been presenting different approaches. One of the most frequent is the use of 3D printers, since this kind of device became popular in the last years. A very complete study was published by Filippou&Tsoumpas (Filippou and Tsoumpas, 2018) which shows the huge potentiality of this kind of technology applied to phantom manufacture. For example, in a recent study presented by Zhang et al. (2018) the authors propose a very realistic anthropomorphic heterogeneous mouse phantom for multimodality medical imaging. The developed device can be used for CT, MRI and PET technologies. In the same field of combine 3D printer technology with the possibility of construction multimodality phantoms, He et al. (2019) shows very interesting results of an anthropomorphic breast phantom. These works, however focus more on the construction methods and results for image quality evaluation them on the transmission properties of the constituent materials in the range of energy of interest for each king of clinical application.

Exception of this fact are the works presented by Ivanov et al. (2018), who evaluated the applicability of low density materials for 3D printer construction of breast phantoms. In this paper, the authors show a very sophisticated and detailed experimental work for the determination of attenuation and refractive properties of materials compatible with 3D printer technology and compare these properties to adipose, glandular and skin tissues. Dahal et al. (2018) also shows an innovative approach using gelatin-based using the concept of tunable x-ray attenuation properties, also focusing 3D printer technology. Although important for understand the availability of different materials and methods for tissue equivalent development, these works no not provide consistent information which allows comparative evaluations in terms

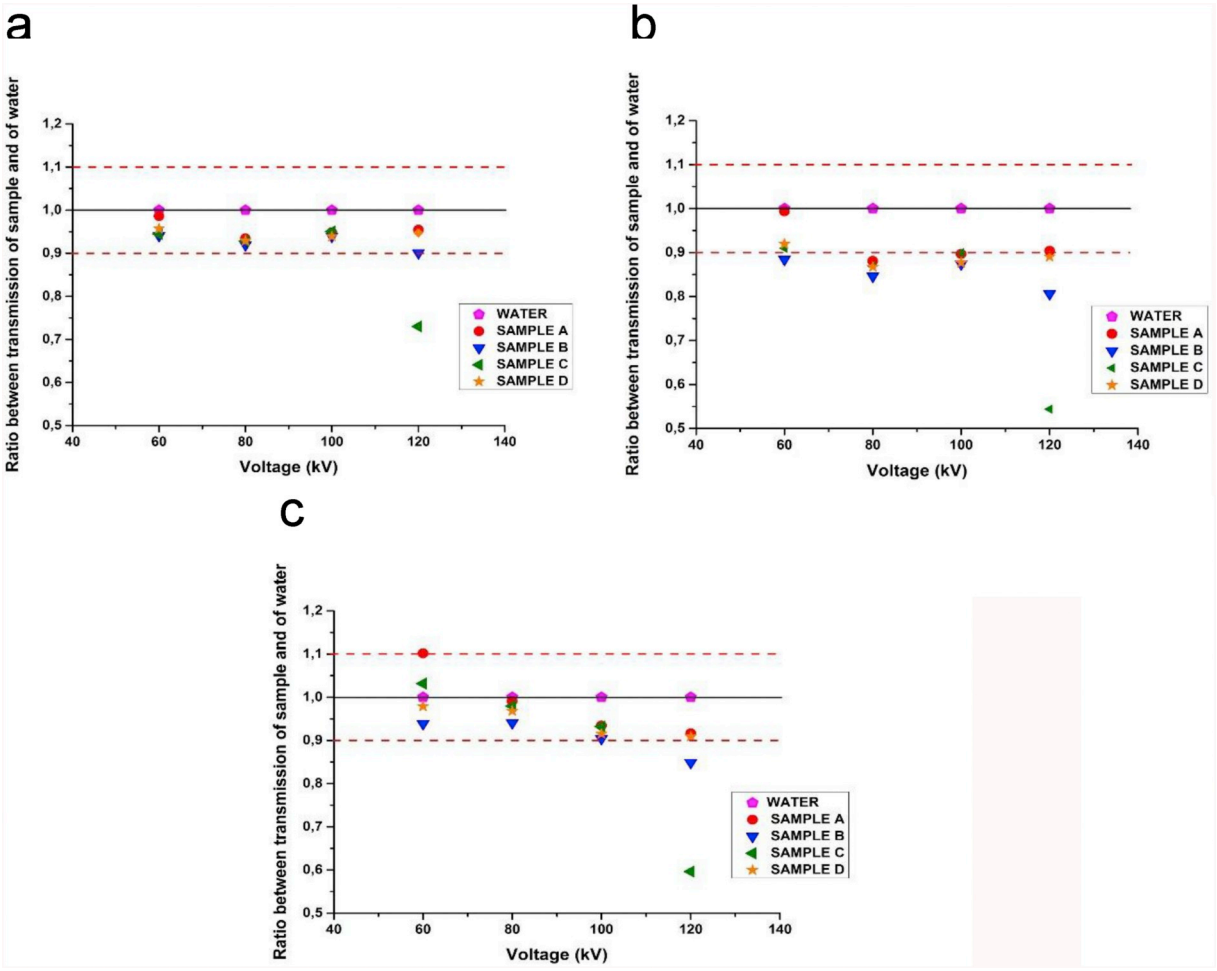

Fig. 5. Comparison between the transmissions of the samples and water for values of thicknesses of (a) 10 mm, (b) 30 mm and (c) 60 mm. Red dashed lines represent the range of ± 10%. (For interpretation of the references to colour in this figure legend, the reader is referred to the Web version of this article.)

Table 3
Equivalency between water thickness and samples thicknesses for a tension of 100 kV.

	Transmission factor	Ratio between the sample thickness and the water thickness			
		Sample A	Sample B	Sample C	Sample D
60 kV	**0.4**	1.00(2)	0.87(2)	0.90(2)	0.91(2)
	0.6	0.97(4)	0.83(3)	0.85(3)	0.88(3)
	0.8	0.92(8)	0.79(7)	0.80(7)	0.84(7)
80 kV	**0.4**	0.88(2)	0.84(2)	0.86(2)	0.87(2)
	0.6	0.80(3)	0.75(3)	0.79(3)	0.79(3)
	0.8	0.74(6)	0.71(5)	0.72(6)	0.73(6)
100 kV	**0.4**	0.89(2)	0.86(1)	0.80(1)	0.86(2)
	0.6	0.83(3)	0.79(2)	0.73(2)	0.79(2)
	0.8	0.79(5)	0.75(5)	0.69(5)	0.75(5)
120 kV	**0.4**	0.89(1)	0.77(1)	0.45(1)	0.87(1)
	0.6	0.84(2)	0.69(2)	0.38(2)	0.81(2)
	0.8	0.80(5)	0.63(5)	0.34(4)	0.78(5)

Table 4
Table of the determined values of density of the samples and the given value of density of water.

	Density (g/cm^3)
Sample A	1.1519(1)
Sample B	1.1437(1)
Sample C	1.1407(1)
Sample D	1.1444(1)
Water	0.9969(1)

of important properties, such as effective atomic number and electron density, neither regarding availability and production costs.

On the other hand, Amini et al. (2018) present a very consistent study of tissue equivalent materials for CT phantoms. These authors presented physical properties such as mass density, electron density and effective atomic number of a wide range of available polymers and compared these properties with the target tissues. Comparing the values listed by Amini et al. with those presented here, it can be seen that the effective atomic number of the equivalent materials developed in this work is closer to that of Solid Water. In terms of electronic density, Teflon has the more equivalent value comparing with samples A, B, C and D. Akhlaghi et al. (2015) also show similar properties of several materials, focusing in the construction of a 8 years-old CT dosimetric phantom. In this case none of the UF original tissues values of atomic number approaches with those of the samples developed in the present study. On the other hand, the values of electronic density of materials A-150, PMMA and Polycarbonate are close to the electronic densities of our materials.

The samples developed and studied in the present work were designed to be equivalent to the water, considering its abundance in the human body. Our experimental findings in terms of thickness, mass and electron density and effective atomic number links the applications of the materials to potential applications in clinical practices where human body are water-rich, such as organs with predominance of soft tissues (abdominal organs, breast, muscles etc.).

The samples were evaluated in terms of their transmission properties assuming diagnostic range of energies, excluding mammography.

Complementary studies have been done in order to evaluate these materials using spectrometric approaches (Frimaio et al., 2019). Additionally, other experimental method can be potentially adopted in order to improve the qualification of these samples for other ranges of energies, such as that used in breast imaging. Finally, the authors are planning to investigate the developed materials focusing new imaging technologies such as spectral imaging (referencia do Fredenberg e do Lee) e contrast-enhanced techniques (Bliznakova et al., 2016a,b).

4. Conclusion

Materials made of resin compounds were submitted to radiation transmission tests for phantom development. Four samples were evaluated and the results indicated that the better correspondence between the developed materials and the water in terms of scattering and transmission properties were for the lowest values of thicknesses (10 mm and 30 mm) and the lowest values of transmission factors (0.4 and 0.6). The lowest percentage difference between the water transmission and the transmission of any of the samples obtained was approximately 0.6% for the sample A in the thickness of 30 mm under voltage of 60 kV. Therefore, sample A was the one that best represents the water in the range of tension studied. Sample C was the most different from water in terms of transmission of radiation, especially under a voltage of 120 kV. Due to the significant agreement between the thicknesses of the samples and of water, it was verified that it is possible to develop national phantoms with the compounds studied in this paper.

Acknowledgements

The authors would like to thank the support of National Council for Scientific and Technological Development (CNPq) and Foundation for Research Support of the State of São Paulo (FAPESP) by project Metrology of Ionizing Radiation in Medicine (INCT) (process 573659/2008-7). In addition, authors wish to acknowledge the technicians Marcos S. de Souza and Claudio H. Furukawa for the support in confection and density measurement of the samples.

References

Akhlaghi, P., Hakimabad, H.M., Motavalli, L.R., 2015. Determination of tissue equivalent materials of a physical 8-year-old phantom for use in computed tomography. Radiat. Phys. Chem. 112, 169–176.

Amini, I., Akhlaghia, P., Sarbakhsh, P., 2018. Construction and verification of a physical chest phantom from suitable tissue equivalent materials for computed tomography examinations. Radiat. Phys. Chem. 150, 51–57.

Archer, B.R., Fewell, T.R., Conway, B.J., Quinn, P.W., 1994. Attenuation properties of diagnostic X-ray shielding materials. Med. Phys. 21, 1499–1507.

Archer, B.R., Thornby, J.I., Bushong, S.C., 1983. Diagnostic X-ray shielding design based on an empirical model of photon attenuation. Health Phys. 44, 507–517.

Burguer, A., Costa, P.R., Archer, B.R., IOMP, 2011. Exploring the parameters of a widely used mathematical model of X ray transmission. In: International Conference on Medical Physics. Porto Alegre. IOMP, RS, Brasil.

Bliznakova, K., Mettivier, G., Russo, P., Buliev, I., 2016a. Contrast Detail Phantoms for X-Ray Phase-Contrast Mammography and Tomography. Breast Imaging: 13th International Workshop, IWDM 2016, Malmö, Sweden, June 19-22, 2016, Proceedings In: Tingberg, A., Lång, K., Timberg, P. (Eds.), Springer International Publishing, Cham, pp. 611–617.

Bliznakova, K., Russo, P., Kamarianakis, Z., Mettivier, G., Requardt, H., Bravin, A., Buliev, I., 2016b. In-line phase-contrast breast tomosynthesis: a phantom feasibility study at a synchrotron radiation facility. Phys. Med. Biol. 61 (16), 6243–6263.

Caballo, M., Mann, R., Sechopoulos, I., 2018. Patient-based 4D digital breast phantom for perfusion contrast-enhanced breast CT imaging. Med. Phys. 45 (10), 4448–4460.

Constantinou, C., Attix, F.H., Bhudatt, M.S., et al., 1982. A solid water phantom material for radiotherapy X-ray and gamma-ray beam alibrations. Med. Phys. 9, 436–441.

Costa, P.R., 2015. Overview of Medical Physics Teaching in Brazil. Research on Biomedical Engineering.

Costa, P.R., Caldas, L.V.E., 2002. Evaluation of protective shielding thickness for diagnostic radiology rooms: Theory and computer simulation. Med. Phys. 29 (1), 73–85.

Dahal, E., Badal, A., Zidan, A., Alayoubi, A., Hagio, T., Glick, S., Badano, A., Ghammraoui, B., 2018. Stable gelatin-based phantom materials with tunable x-ray attenuation properties and 3D printability for x-ray imaging. Phys. Med. Biol. 63, 09NT01.

Dewerd, L.A., Lawless, M., 2014. Introduction to phantoms of medical and health physics. In: Dewerd, A.L.K.,M. (Ed.), The Phantoms of Medical and Health Physics. Springer, New York.

Filippou, V., Tsoumpas, C., 2018. Recent advances on the development of phantoms using 3D printing for imaging with CT, MRI, PET, SPECT, and ultrasound. Med. Phys. 45 (9), 40–760.

Fisher, R.F., 2006. Tissue Equivalent Phantoms for Evaluating In-Plane Tube Current Modulated CT Dose and Image Quality (MS Thesis). University of Florida, FL, USA, pp. 1–78.

Frimaio, A., 2017. Pesquisa e Desenvolvimento de Compostos Termoplásticos e/ou Termofixos Equivalentes ao Tecido Humano. Universidade de São Paulo, São Paulo.

Frimaio, A., Nascimento, B.C., Barrio, R.M.M., Campos, L.L., Costa, P.R., 2019. X-ray spectrometry applied for determination of linear attenuation coefficient of tissue-equivalent materials. Radiat. Phys. Chem. 160, 89–95.

Glick, S.J., Ikejimba, L.C., 2018. Advances in digital and physical anthropomorphic breast phantoms for x-ray imaging. Med. Phys. 45 (10), 870–885.

He, Y., Liu, Y., Dyer, B.A., Boone, J.M., Lui, S., Chen, T., Zheng, F., Zhu, Y., Sun, Y., Rong, Y., Qiu, J., 2019. 3D-printed breast phantom for multi-purpose and multi-modality imaging. Quant. Imag. Med. Surg. 9 (1), 63–74.

IAEA, 2007. Dosimetry in Diagnostic Radiology: An International Code of Practice. Technical Reports Series No. 457. International Atomic Energy Agency, Vienna, Austria (International Atomic Energy Agency).

IAEA, 2011. Implementation of the International Code of Practice on Dosimetry in Diagnostic Radiology (TRS 457): Review of Test Results. Viena.

ICRU, 1989. Tissue substitutes in radiation dosimetry and measurement (ICRU report No. 44). Int. Comm. Radiat. Units Meas.

International Commission on Radiological Protection (ICRU) No. 23, 1975. Report of the Task Group on Reference Man.

Ikejimbaa, L.C., Graff, C.G., Rosenthal, S., Badal, A., Ghammraoui, B., Lo, J.Y., Glick, S.J., 2017. A novel physical anthropomorphic breast phantom for 2D and 3D x-ray imaging. Med. Phys. 44 (2), 407–416.

Ivanov, D., Bliznakova, K., Buliev, I., Popov, P., Mettivier, G., Russo, P., Di Lillo, F., Sarno, A., Vignero, J., Bosmans, H., Bravin, A., Bliznakov, Z., 2018. Suitability of low density materials for 3D printing of physical breast phantoms. Phys. Med. Biol. 63, 175020.

Kimura, B.H., Frimaio, A., Costa, P.R., 2011. Development of tissue equivalent polymeric composites: preliminary results. Porto Alegre: Anal. Int. Conf. Med. Phys.

Manohara, S.R., Hanagodimath, S.M., Thind, K.S., Gerward, L., 2008. On the effective atomic number and electron density: A comprehensive set of formulas for all types of materials and energies above 1keV. Nucl. Instrum. Methods Phys. Res. Sect. B Beam Interact. Mater. Atoms 266, 3906–3912.

Mariano, L., 2017. Desenvolvimento de uma metodologia para formulação de materiais radiologicamente equivalentes ao tecido humano. Universidade de São Paulo, São Paulo.

Mariano, L., Costa, P.R., 2017. Development of a methodology for formulating radiologically equivalent materials to human tissues. In: Russo, P. (Ed.), International Conference on Monte Carlo Techniques for Medical Allications. Elsevier, Napoles.

Prasad, S.G., Parthasaradhi, K., Bloomer, W.D., 1997. Effective atomic numbers of composite materials for total and partial interaction processes for photons, electrons, and protons. Med. Phys. 24, 883–885.

Saito, M., Sagara, S., 2017. A simple formulation for deriving effective atomic numbers via electron density calibration from dual-energy CT data in the human body. Med. Phys. 44, 2293–2303.

Santos, J.C., Tomal, A., Mariano, L., Costa, P.R., 2015. Application of a semi-empirical model for the evaluation of transmission properties of barite mortar. Appl. Radiat. Isot. 100, 38–42.

Shrimpton, P.C., 1981. Electron density values of various human tissues: in vitro Compton scatter measurements and calculated ranges. Phys. Med. Biol. 26, 907–911.

Taylor, M.L., Smith, R.L., Dossing, F., Franich, R.D., 2012. Robust calculation of effective atomic numbers: The Auto-Zeff software. Med. Phys. 39, 1769.

Tomal, A., Costa, P.R., 2017. Phantoms for Image Quality and Dose Assessment. Handbook of X-Ray Imaging: Physics and Technology. vol. 4 CRC Press, P. Russo. London chap. 56.

Zhang, H., Hou, K., Chen, J., Dyer, B.A., Chen, J.-C., Liu, X., Zhang, F., Rong, Y., Qiu, J., 2018. Fabrication of an anthropomorphic heterogeneous mouse phantom for multi-modality medical imaging. Phys. Med. Biol. 63, 195011.